Journal of Food Measurement and Characterization (2024) 18:7728–7738
https://doi.org/10.1007/s11694-024-02760-y

ORIGINAL PAPER

Micromechanical characterization of a wheat-based food material as a function of moisture content

Karla Cecilia Cisneros Martinez[1] · Ramin Nemati[2] · Pawan Singh Takhar[1]

Received: 18 April 2024 / Accepted: 9 July 2024 / Published online: 24 July 2024
© The Author(s), under exclusive licence to Springer Science+Business Media, LLC, part of Springer Nature 2024

Abstract

The microstructural changes in food materials during the baking process directly influence their micromechanical properties and, thus, the strength of the solid walls. Baking time, as one of the vital variables, impacts the microstructural and micromechanical characteristics, alters the texture, and affects customer satisfaction. This research aims to investigate the alteration in three critical micromechanical properties: hardness, stiffness, and Young's modulus, as a function of moisture content during baking of cookies in an oven set at 185 ± 1 °C in the range of 10 to 60-min. The nanoindentation method, which involves pushing a nanoindenter into and removing it from cookie samples to measure the force-displacement data, was employed to measure the micromechanical properties. The results indicated that all the micromechanical properties initially increased when the moisture content decreased from 12.26 to 8.53 g/100 g solids and showed fluctuating trends at the later moisture content values. Throughout the baking process, the moisture content ranges from 2.71 to 12.26 g/100 g solids. Simultaneously, hardness varies from 0.28 to 0.88 GPa, stiffness ranges between 9.77 and 20.16 µN/nm, and Young's modulus experiences minimum and maximum values of 4.34 and 14.55 GPa, respectively. Finally, the Analysis of Variance and Duncan's multiple range tests revealed a significant difference between the mean values of some data points of hardness, stiffness, and Young's modulus as a function of moisture content.

Keywords Nanoindentation · Hardness · Stiffness · Young's modulus · Cookie

Introduction

Mechanical properties of food materials play a crucial role in the quality of food products and, ultimately, customer satisfaction. However, these characteristics are not constant and can be affected by food processing parameters such as time and temperature. Baked products made from dough are an important example of food products whose characteristics considerably evolve throughout processing. During baking, several chemical, physical, and biochemical alterations, such as water evaporation, protein denaturation, starch gelatinization, Maillard reaction, and volume expansion, take place in the dough matrix and affect its final mechanical properties [1]. Lucas [2] discussed that the changes in bakery products start with the rise of temperature and vaporization of gases. Increased temperature results in starch gelatinization and protein coagulation, which affect cell growth, while gas vaporization leads to an increase in the gas cell volume.

Generally speaking, quality attributes include various measurable characteristics, including structural, optical, textural, thermal, sensory, nutritional, and rehydration properties [3]. One of these attributes, food texture, which is related to the structural and mechanical properties of food materials, plays a crucial role in affecting consumer perception of quality and taste [4, 5]. In addition, studies have shown that the texture of food and, thus, consumer appeal of products are intricately connected to the microstructure of products within the range of 0.1–100 µm [6]. Microstructure can be described as the arrangement and interaction of elements across the material phases. For baked foods, these elements include starch granules, proteins, water, gas bubbles,

Author PST has previously published as Pawan P. Singh.

✉ Pawan Singh Takhar
ptakhar@illinois.edu

1 Food Science and Human Nutrition, University of Illinois at Urbana-Champaign, Urbana, IL 61801, USA

2 Agricultural and Biological Engineering, University of Illinois at Urbana-Champaign, Urbana, IL 61801, USA

and fat crystals, which contribute to the final product texture profile [7]. Since microstructure transformation takes place below 100 µm, nanoindentation seems to be a promising technique to determine the micromechanical properties of food materials. Its small probe size also enables the nanoindentation method to investigate small samples with a thin depth and heterogeneous structure, which are challenging to explore through traditional mechanical testing techniques [8]. Besides, for composite samples consisting of two or more materials with different physical properties, nanoindentation allows measuring the properties of individual materials [9].

Nanoindentation involves applying a continuous force to a designated spot on the test sample to deform it by nano-to-microscale depth [10]. Using an indenter tip of a known area and analyzing the loading-unloading curve (also known as the force-displacement curve), one can obtain the hardness, stiffness, Young's modulus, and other mechanical properties of materials [11]. Hardness refers to the evaluation of a material's resistance to plastic deformation in a specific region of the sample [12]. Stiffness is defined as the ability of a material to resist deformation under tensile or compressive loading [13]. A material's Young's modulus, on the other hand, is directly related to its stiffness and describes a material's resistance to elastic deformation [14]. With micromechanical properties in hand, it becomes possible to acquire valuable information about the strength of solid walls and determine a product's cracking proneness. The importance of this information lies in the fact that thinner solid walls have a higher possibility of crumbling into powder during processing or inside the food package, shipping or storage [15, 16]. As an important indication of wall thickness, higher Young's modulus values imply lower changes in shape and higher resistance to deformation under a load, therefore, higher strength of the cell walls [17].

The area under a nanoindentation curve provides valuable information about plastic and elastic work (Fig. 1a). The total work done during loading can be divided into irrecoverable and recoverable energies. The area enclosed by points O, B, and C (D1) represents the irrecoverable energy (plastic work or plastic deformation energy). Conversely, D2, which corresponds to the area enclosed by points C, B, and A, represents the recoverable energy (elastic work) recovered during unloading [18–22]. Hysteresis observed in nanoindentation differs from that in other nanomechanical tests. For instance, in the Atomic Force Microscopy (AFM) process (see Fig. 1b), attractive forces push the cantilever (moves from right to left) until the maximum load is reached [23, 24]. The cantilever is then retracted from the sample (moves from left to right), overcoming adhesion forces until it returns to equilibrium. During this retraction process, the deformation that recovers is termed elastic deformation, while the deformation that does not recover is termed plastic deformation [25]. The area between the baseline and the retraction curve represents the energy dissipation or work of adhesion of the material [26, 27]. Nanoindentation and AFM are both nanomechanical tests in which a probe applies a specified force to a sample surface to measure its properties. However, the nanoindenter tips, with a radius of several hundred nanometres, are larger than AFM tips, which have a radius of about ten nanometres. This difference poses challenges in determining the shape and dimensions of AFM tips, thereby influencing the obtained results [28]. Moreover, AFM probes are highly sensitive and often consumable during their interaction with the surface, requiring accurate characterization of their geometry for each experiment [29]. These issues complicate the quantification of measurements compared to nanoindentation methods. Additionally, nanoindentation is preferred when upscaling to macroscale properties because the modulus measured by

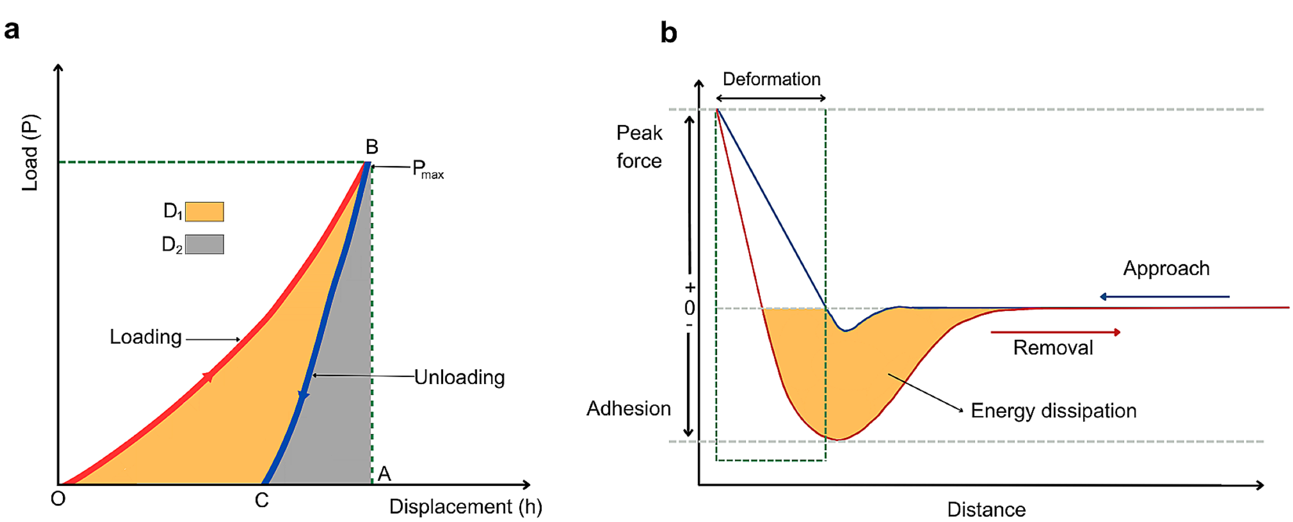

Fig. 1 Representation of work done in (**a**) the nanoindentation and (**b**) AFM processes (Adapted from [18, 23])

this method is more influenced by the interaction of aggregates rather than individual particles being probed [30].

The nanoindentation-based method has been widely applied in material science, with a recent interest in food science to determine micromechanical properties. An example is the study of Zdunek and Kurenda, [31] in which they successfully characterized the micromechanical proprieties of tomato fruit cells in pericarp by employing the AFM-based nanoindentation method. By evaluating Young's modulus, they were able to address postharvest cell degradation. Similarly, Khodabakhshian et al. [32] obtained elastic modulus and stiffness in banana mesocarp cells, demonstrating the capacity to determine the nanomechanical properties of isolated cells with AFM-based nanoindentation. Another study was performed in pear cells to investigate the postharvest influence on micromechanical proprieties, specifically during refrigeration to shelf-life conditions at 20 °C [33]. AFM-based nanoindentation technique was also employed by Cárdenas-Pérez et al. [34] to ascertain the nanomechanical proprieties of apple cells and tissues. This investigation centered on characterizing tissue surface properties and revealed that apple cells within the tissue exhibited a higher Young's modulus compared to their isolated counterparts. Moreover, the nanoindentation technique proved to be helpful in analyzing characteristic changes during ripening and finding out the relation between firmness and Young's modulus [35]. Edible films' micromechanical properties have also been studied using nanoindentation. Escamilla-García et al. [36] employed nanoindentation to characterize the proprieties of zein and chitosan edible films. The objective was to discern elasticity and hardness variations in five formulations of zein and chitosan. In another research, modified starch-chitosan edible films have been characterized with nanoindentation to determine the mechanical properties of different formulations of modified starch and chitosan within thin films [37]. Nanoindentation has been used in the elaboration of elastic modulus mapping of several sections of hen's eggshells, for which local variations in shell elastic modulus were determined [38]. Additionally, this technique has been successfully applied to characterize the micromechanical properties of plant-based foods as a function of drying variables. For instance, Dhalsamant et al. [39] applied nanoindentation tests to determine the influence of pre-heat treatment over solar-dried potato cylinders, resulting in higher reduced and Young's modulus compared to the non-pre-heated samples. In another research effort, Khan et al. [40] established the relationship between the micromechanical properties (Young's modulus, hardness, and stiffness) and moisture content of cylindrical slices of carrots during drying in a multi-tray cabinet dryer, finding a significant increase in the magnitude of these properties with the reduction in moisture content toward end of drying.

To our knowledge, there is an absence of the application of the nanoindentation method in wheat-based baked products. Therefore, the primary aim of this study is to investigate the solid wall micromechanical properties of cookies, a widely consumed cereal-based food, using the nanoindentation method. It focuses on measuring various micromechanical properties, including stiffness, hardness, and Young's modulus at different moisture content values. One-way ANOVA and Duncan's multiple range test are employed to analyze differences between means in the collected data. The results of this study will offer valuable insights to the cookie industry, enabling them to improve product quality and texture.

Table 1 Ingredients for dough preparation

Ingredients	Quantity (g)	Quantity (%)
All-purpose flour	180	37.11
Granulated sugar	134	27.63
Coconut oil	113	23.3
Pasteurized egg white	50	10.31
Salt	4	0.82
Baking powder	4	0.82

Materials and methods

Sample preparation

Cookies were prepared using the ingredients listed in Table 1. Meijer brand all-purpose flour composed of bleached wheat flour, niacin, reduced iron, thiamine mononitrate, riboflavin, folic acid, and enzymes were utilized. According to the nutrition label, based on a 30 g serving size, the product comprises 0 g of fat, 0 mg of cholesterol, 0 mg of sodium, 23 g of carbohydrates (including less than 1 g of fiber and 0 g of sugar), and 3 g of protein. Each ingredient was accurately measured using an FX-3000i precision balance (A&D Co. Ltd., Tokyo, Japan) with a tolerance of ± 0.05 g. Afterward, the sugar, coconut oil, and egg whites were placed in a bowl to be mixed with an electric flat beater until a milky solution was obtained. Next, the dry ingredients were mixed in a separate container and incorporated slowly with a spoon into the milky solution, mixing between each addition to ensure homogeneity.

In the subsequent step, the dough was rolled out on a flat surface until it reached a thickness of 12 mm. A circular stainless steel cookie cutter of 6 cm diameter was used to cut disk shapes. To ensure the correct thickness of 12 mm, every dough circle was measured using a vernier scale. The samples were placed in individual aluminum cans with parchment papers on the bottom, ensuring uniform heat distribution. Aluminum cans with no lids were then placed in a preheated Isotemp 6901 oven (Thermo Fisher Scientific Inc.,

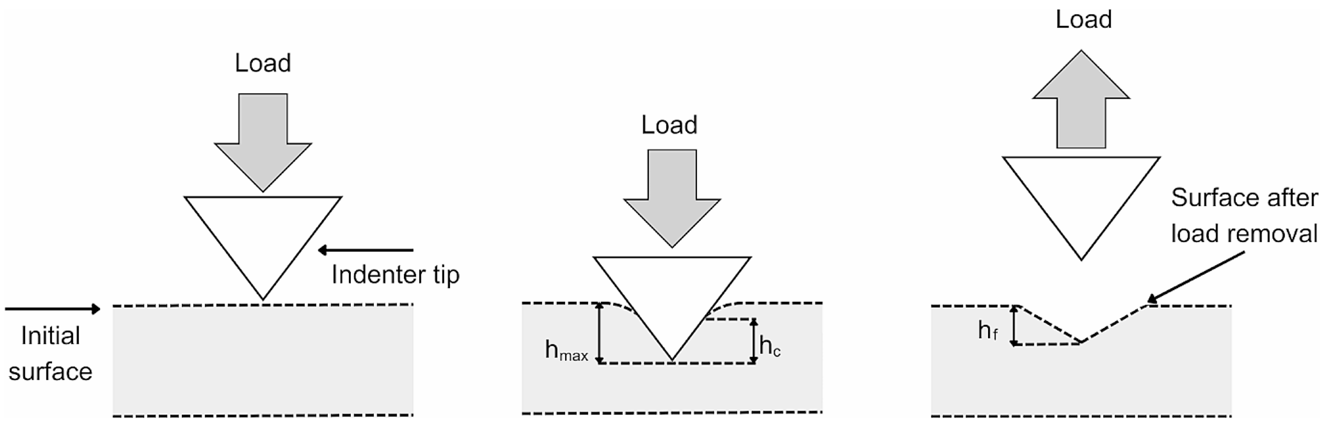

Fig. 2 Schematic representation of a typical nanoindentation process: (**a**) indenter approaching the untouched surface, (**b**) gradual increase in load until reaching the maximum load and depth, and (**c**) irreversible surface deformation formed after unloading (Adapted from [41, 42])

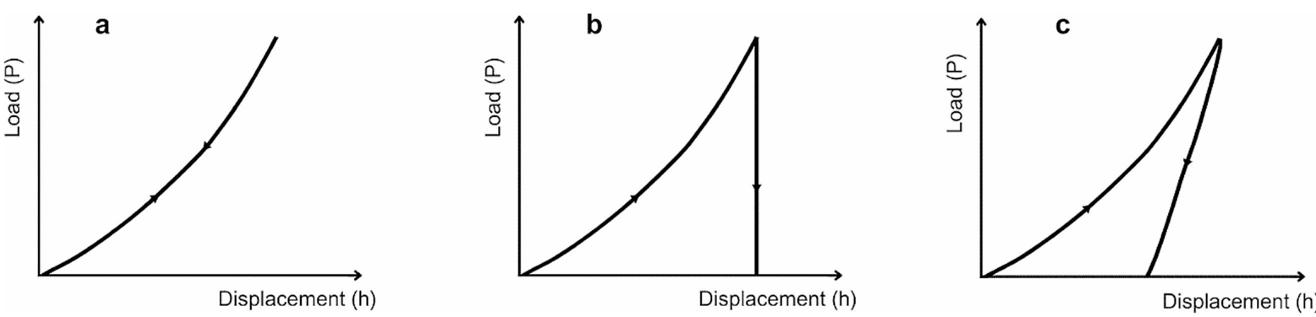

Fig. 3 Schematic representations of load-displacement curves for different materials: (**a**) elastic solid, (**b**) ideally plastic material, (**c**) elastic-plastic material (Adapted from [10, 18])

Waltham, MA, USA) with a temperature set at 185 ± 1 °C monitored with a thermocouple. A total of eleven different baking times were tested to obtain their corresponding moisture content values ranging from 10 to 60 min, with a 5-minute interval between each test. The samples taken out of the oven at a given baking time were hermetically sealed in aluminum cans to prevent moisture loss.

To prepare the baked cookie samples for the nanoindentation tests, they were sliced into cubic shapes with a cross area of 1.5 cm × 1 cm using a scalpel. A cookie's height undergoes fluctuations during baking because of expansion and contraction phenomena. As a result, the height of the samples is not constant throughout the process. The cubes were subsequently sanded to achieve a smooth and even surface, which is required to prevent the tip from crashing during the nanoindentation process. Initially, a coarse sandpaper with a grit size of 220 was employed to scrape off the larger uneven shapes on the cookie surface. This helped to prepare the surface for extra sanding with higher grit number sandpapers. A sequence of five micro-abrasive paper grids, including 7000, 8000, 10,000, 12,000, and 15,000, was then used to ensure a smooth surface.

Nanoindentation experiments

Nanoindentation is a method that involves applying a load to a sample to deform it at a micron scale. A remarkable feature of this test is the indirect measurement of the contact area by the indenter penetrating at small scales. In a typical nanoindentation test, an indenter with a defined geometry is first driven into the surface of the testing material (Fig. 2a), where the elastic deformation begins [10, 41]. The load increases steadily at a constant rate until the pre-determined maximum load is attained (Fig. 2b). h_{max} represents the maximum displacement, and h_c (also called contact depth) denotes the vertical distance between the location of the tip of the indenter and the separation point between the indenter and the surface of the sample. Once the peak is reached, the unloading cycle begins. Here, the material recovers partially from the elastic deformation but leaves an irreversible plastic deformation on the surface called indentation (h_f), shown in Fig. 2c [42–45].

By pushing the indenter into and removing it from the sample and monitoring the applied load and indenter tip displacement, one can obtain loading and unloading curves known as cycles [46]. Figure 3 represents a schematic representation of load-displacement curves for different materials under the nanoindentation process. The unloading curve matches the loading curve for perfectly elastic materials (Fig. 3a). For ideally plastic materials (Fig. 3b), unloading curves are presented as straight lines perpendicular to the displacement axis. Figure 3c exhibits the behavior of a material with both elastic and plastic deformation. After the load removal, this material experiences some elastic recovery [10, 18, 47].

The loading-unloading curves for a material with both plastic and elastic deformation are shown in Fig. 4 in more detail. The loading curve, represents the continuous displacement of the tip through the sample until the set maximum load (P_{max}) is reached. In this study, a maximum load of 1 μN was set to obtain a displacement resolution of approximately 200 to 450 nm. The unloading curve represented in Fig. 4can be obtained when the force is removed from the sample, allowing the sample to recover partially. Stiffness (S) is then calculated by the slope of the force-displacement curve upon unloading [10, 48].

As with other effective parameters, the material used in a nanoindenter and the nanoindenter shape influence the nanoindentation result. The indenters are usually made of sapphire or diamond. In addition, the most common shapes in indenters are spherical, Vickers, Berkovich, cube corner, and Knoop. Among these, the Berkovich three-sided pyramid diamond tip is considered versatile because of its sharp form and constant area-to-depth ratio, which make it suitable for hard and soft materials [49]. In this study, the nanoindentation experiments were conducted using a Berkovich indenter tip with a face angle (the angle between the center line and the three faces) of θ = 65.27° [50–52].

The nanoindentation experiments were carried out with the nanoindenter Hysitron TI 950 TriboIndenter (Hysitron, Inc. Minneapolis, MN, USA) available in the Material Research Laboratory at the University of Illinois at

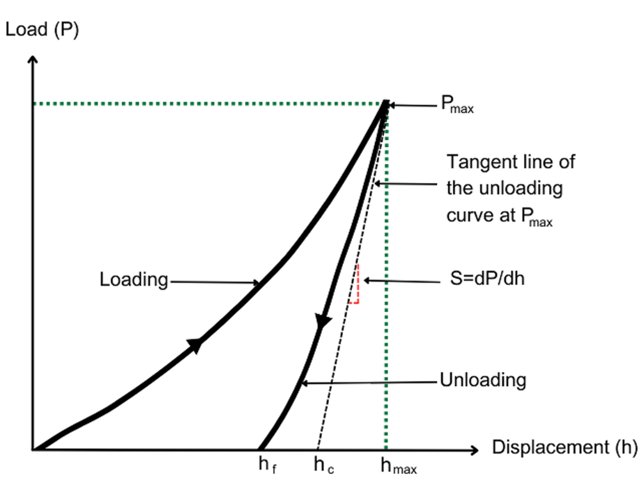

Fig. 4 Representation of loading and unloading curve during the nanoindentation process (Adapted from [10, 48])

Urbana-Champaign. To avoid movement during the indentation, the samples were mounted on magnetic AFM discs, and then superglue was utilized to form strong bonds between the sample and the disc surface. Given the complexity of the cookie matrix and its uneven surface structure, the nanoindentation experiment was replicated 12 times at each baking time. Four samples were extracted from each cookie, and the indentation experiment was conducted in 3 different spots on each of those samples to obtain a total of 12 readings per baking time.

The equations used to calculate hardness and the contact area are the following [42–44, 53, 54]:

$$H = \frac{P_{max}}{A} \tag{1}$$

$$A = 24.56h_c^2 \tag{2}$$

In Eq. 1, H is hardness, P_{max} is the maximum load in the indentation test, and A is the Berkovich tip contact area which can be obtained using Eq. 2, where h_c represents the contact depth.

To determine the elastic modulus or Young's modulus of the samples, it is required to calculate the reduced modulus (E_r) first. This can be calculated by employing:

$$E_r = \frac{\sqrt{\pi}}{2\beta}\frac{S}{\sqrt{A}} \tag{3}$$

Here, β is the geometric correction for the Berkovich tip ($\beta = 1.034$), S is stiffness, π is the mathematical constant, and A is the contact area. The sample's Young's modulus can then be calculated using:

$$E = \left(1 - v^2\right)\left(\frac{1}{E_r} - \frac{1 - v_I^2}{E_I}\right)^{-1} \tag{4}$$

where E is Young's modulus, E_r is the reduced elastic modulus, v_I is the diamond tip's Poisson's ratio having the numerical magnitude of 0.07, E_I is the Young's modulus of the diamond indenter tip with a value of 1140 GPa, and v is the sample's Poisson's ratio. According to Finney [55], the Poisson's ratio for food materials is typically between 0.3 and 0.5. However, in this case, a value of 0.22 was used to estimate Young's modulus of the cookie samples, which corresponds to Poisson's ratio of wheat [56].

Moisture content determination

The sample's moisture content was determined by the AACC [57] method number 44-15.02 with some modifications. Prior to weighing the samples, the aluminum cans were dried in a Fisher Scientific PR305225G gravity convection oven at 105 ± 1 °C for 8 h and then cooled in a desiccator for an hour. Following cooling, the weight of each can and its corresponding lid was recorded using an analytical balance, and then 10 ± 0.005 g of the ground sample was weighed in triplicate. The samples were dried for 24 h at 105 ± 1 °C and the moisture content values were expressed on a dry basis.

Statistical analysis

The collected data for hardness, stiffness, and Young's Modulus were subjected to analysis of variance (ANOVA) using SAS version 9.4 (SAS Institute Inc. Cary, NC, USA) to determine the significance of the differences at a significance level set at $P < 0.05$. In addition, Duncan's multiple range test (DMRT) was used to measure the specific differences between means and determine which mean values were statistically different or equal to the other mean values.

Software tools

Figures 1, 2, 3 and 4 were created using Canva, online graphics creation tool. Remaining figures were created using Microsoft Excel.

Results and discussion

Temperature evolution near the cookie center as a function of baking time is illustrated in Fig. 5. As expected, by increasing the baking time, the temperature inside the cookie rises and gradually approaches the oven temperature (185 ± 1 °C). The temperature increases rapidly at the initial stage of baking, followed by stabilization, and increases again at the end of the baking process, at which point most of the water is expected to evaporate. This trend is in agreement with the findings presented by Ameur et al. [58]. and Chevallier et al. [59]. Furthermore, the changes in moisture content during the baking process are presented in Fig. 6. It is evident that there is a noticeable decrease in moisture content in the first half of the baking process, from 10 to 30-min, reducing the initial moisture content from 12.26 to 3.89 g/100 g solids. At later baking times of 30 to 55-min, the moisture content remains relatively constant, ranging from 3.86 to 3.37 g/100 g solids. Finally, there is a slight decrease at 60-min with a final moisture content of 2.71 g/100 g solids.

The change in micromechanical properties and moisture content during baking are depicted in Figs. 7, 8 and 9. As can be observed in Fig. 7 the hardness initially experiences a rapid and significant increase when moisture content decreases from 12.26 to 8.53 g/100 g solids and reaches its maximum value of 0.88 ± 0.22 GPa. This trend is expected to have been influenced by moisture loss since moisture content reduction leads to hardness value elevation.

Considering another influencing factor, it can be suggested that movement and content of oil are closely associated with the observed increase in hardness. The fat melts by increasing temperature and moving toward the bottom of the cookie or cookie sides. Decreasing the fat value of food materials, especially on their surface, has been believed to help increase the hardness [60, 61].

Following the first rise in hardness, there is a small decrease from 8.53 g/100 g solids moisture content to 6.41 g/100 g solids moisture content and a noticeable

Fig. 5 Temperature variation near the center of cookies versus time

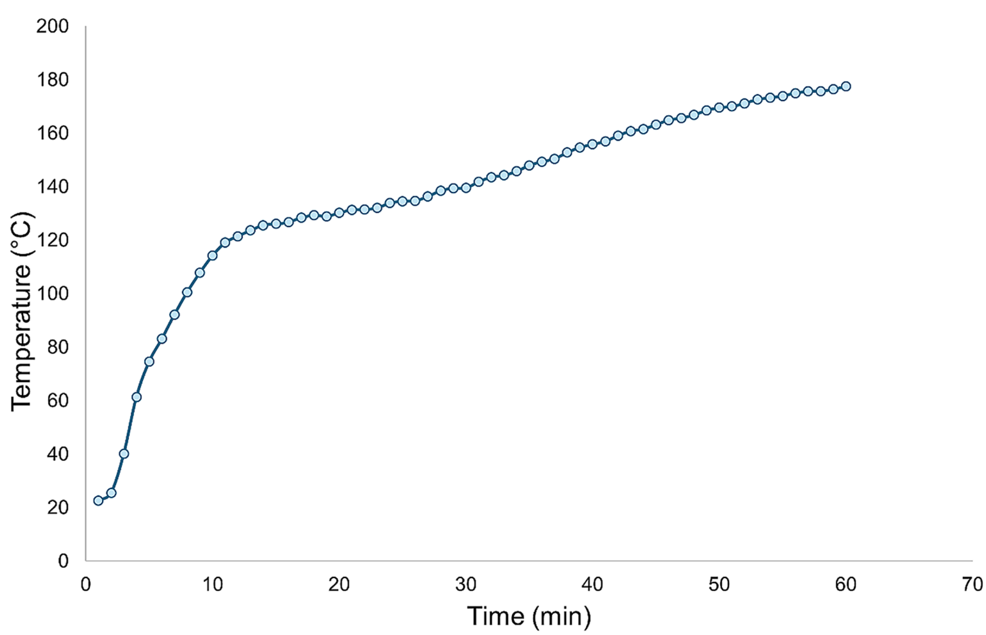

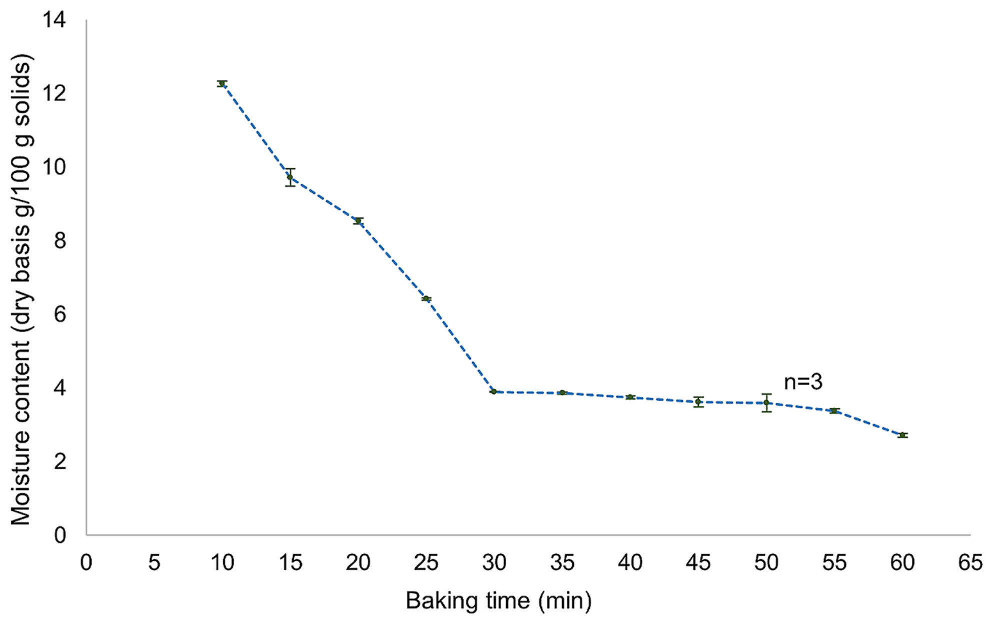

Fig. 6 Moisture content variations on dry basis g/100 g solids as a function of baking time in minutes

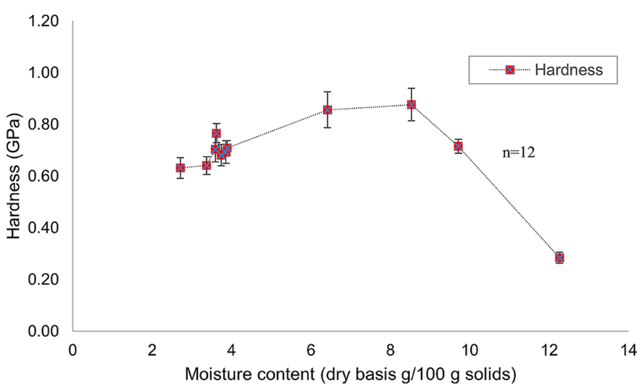

Fig. 7 Hardness variations as a function of moisture content on dry basis (g/100 g solids)

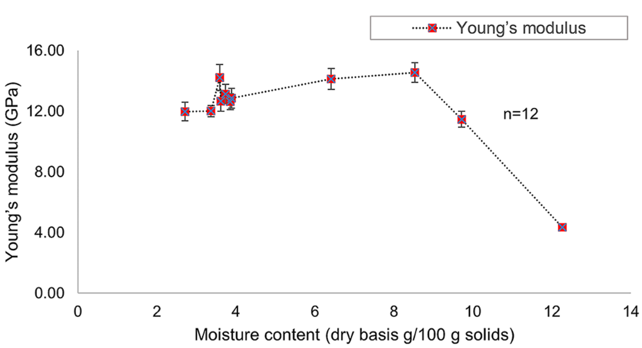

Fig. 8 Young's modulus variations as a function of moisture content on dry basis (g/100 g solids)

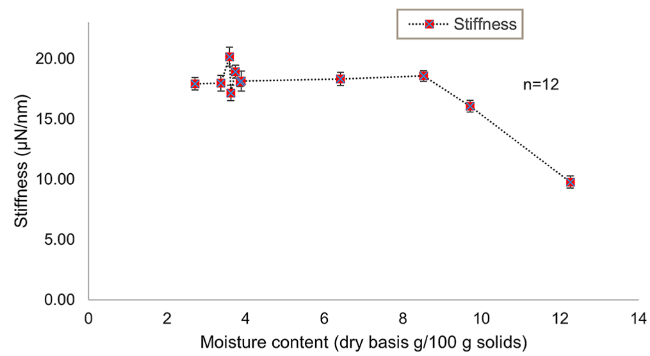

Fig. 9 Stiffness variations as a function of moisture content on dry basis (g/100 g solids)

decrease between 6.41 and 3.89 g/100 g solids. The observed decline in hardness, in the range of 8.53 to 3.89 g/100 g solids moisture content, may be potentially attributed to an increase in porosity. This increase in porosity is expected to result from water evaporation at high temperatures over extended periods, which causes dough expansion during baking. It is expected that by increasing temperature, the baking powder starts to break down into carbon dioxide gas, and water vapors are formed which expand the starch matrix's volume [62, 63]. These two changes raise the cookie dough and increase the porosity. One can expect that by increasing porosity, the solid matrix weakens and consequently leads to a decrease in hardness value. Similar observations on changes in hardness values have been made for the baking of cakes and dried foods [64, 65].

Reduction in hardness continues as moisture content decreases up to 3.74 g/100 g solids. However, between 3.74 and 3.62 g/100 g solids, the hardness increases and reaches a peak value of 0.77 ± 0.13 GPa. The hardness is then reduced along with moisture content in the range from 3.62 to 2.71 g/100 g solids. Measuring hardness at lower moisture levels is crucial to guarantee consistent texture and quality since lower moisture content increases the risk of breakage. Knowledge of the variations in the mechanical properties of foods at different moisture levels allows manufacturers to improve processes and meet regulations and customer preferences. While the change in the hardness value is insignificant during the specific range of moisture content from 3.62 to 2.71 g/100 g solids, there should still be some parameters affecting changes in the hardness value in the mentioned range, such as chemical reaction and pore structure deformation, which could be further investigated in future studies.

It is common sense that the higher the hardness of the cookie, the greater the wall strength. Therefore, cookies with a moisture content of 8.53 and 6.41 g/100 g solids, with hardness values of 0.88 and 0.86 GPa, respectively, have the maximum strength. In future studies, taste acceptability and mouthfeel should be taken into account when selecting the optimum moisture content for a given type of cookie. Too high moisture content is not only perceived as unacceptable from the consumer's perspective but also affects the storage time of cookies [66, 67]. A cookie to be stored safely and to have a crispy texture should have a low moisture content, typically between 1 and 5% on the wet basis, which is equivalent to 1.01–5.26% on the dry basis [68, 69].

The effect of moisture content on Young's modulus is illustrated in Fig. 8. The data shows that Young's modulus initially increases and reaches its first peak of 14.55 GPa at a moisture content of 8.53 g/100 g solids. Then, a declining trend can be observed in the moisture content range of 8.53 to 3.86 g/100 g solids. It reaches the second peak at a moisture content of 3.74 g/100 g solids, with a value of 13.13 GPa.

After a decrease in moisture content from 3.74 to 3.62 g/100 g solids, a notable peak in Young's modulus is observed at 3.59 g/100 g solids. This peak is accompanied by a Young's modulus value of 14.22 GPa. Young's modulus experiences a further decrease in the moisture content values between 3.59 and 3.37 g/100 g solids and remains relatively constant thereafter. It is well understood that higher Young's modulus values indicate lower changes in shape and higher resistance to deformation under a given load, which would cause a higher stiffness of the solid walls [17].

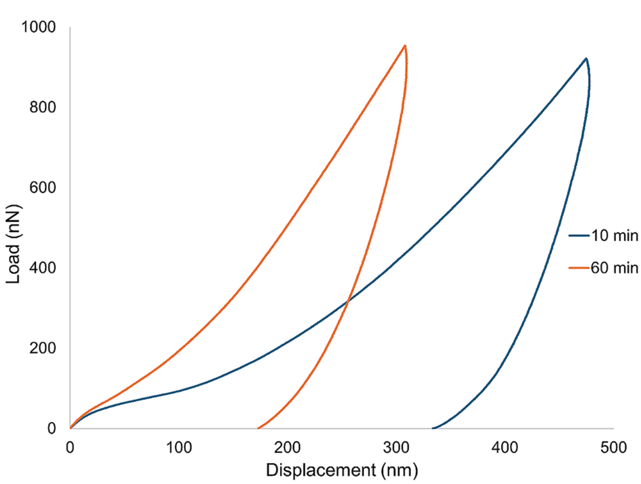

Fig. 10 Loading and unloading curves for cookies baked in 10 and 60 min

Figure 9 demonstrates the impact of moisture content on stiffness. The stiffness and Young's modulus follow a similar trend. In this study, a cookie with a moisture content of 3.59 g/100 g solids is the stiffest, with a stiffness value of 20.16 μN/nm, while the one with a moisture content of 3.74 g/100 g solids, which has a value of 18.91 μN/nm, ranks second. Following the similar reasons as provided above for the hardness value trends, the changes in moisture content, oil content, and development of the porous structure due to CO2 and water vapor generation may account for the trends in the stiffness and Young's modulus curves [2, 59, 70, 71]. For instance, it was demonstrated that the consistent loss of moisture content in a specific range lowers pore water pressure, consequently enhancing the stiffness and Young's modulus [13]. However, the intricate nature of baked products, which arises from the different functions of each ingredient and various chemical and physical alterations that occur during baking, suggests the possibility of other chemical parameters affecting the micromechanical properties of cookies, which were not investigated in this study.

The loading and unloading curves for cookies baked for 10 and 60-min are compared in Fig. 10. Under the same applied load, the maximum penetration depth for the 10-minute sample is greater (475 nm) than for the 60-minute sample (309 nm). According to Mohan [72], a lower indentation depth indicates higher hardness. Therefore, the 10-min sample has lower hardness compared to the 60-min sample. These results are consistent with the hardness values obtained in this study. The area between the loading and unloading curves for the 10-min sample is also greater compared to the 60-min sample, representing higher work done on plastic deformation. This is the irrecoverable energy that is not recovered when the indenter is removed.

One-way ANOVA was conducted to determine significant differences among the means of 11 data groups within the moisture content range of 12.26 to 2.71 g/100 g solids. Considering stiffness as an example, one-way ANOVA compares the mean stiffness values of each moisture content and checks whether the mean values had a significant difference. As one of the comparing criteria, if the p-value is less than the defined significance level (which is selected as 0.05 in this study), the differences between the means are statistically significant, suggesting an influential effect of moisture content on a given property value. Otherwise, one can argue that there is no difference among group means and consequently no relationship between variables, i.e., moisture content is not an influencing parameter for a given micromechanical property. ANOVA shows that the calculated p-values for all the micromechanical properties are less than 0.0001 (Table 2.). By comparing these p-values to the significance level of 0.05, it can be concluded that the mean values of stiffness, hardness, and Young's modulus varied significantly with moisture content and, thus, are influenced by this parameter.

Even though the ANOVA test can establish whether mean values are equal, it does not provide enough information about which means are different. To address this, Duncan's multiple range test (DMRT) was performed post-hoc on the ANOVA test, considering both the degrees of freedom and the number of treatments (Table 3.). To group equal means from other statistically different means, a set of alphabets (a, b, c and d) is assigned to each treatment. If two treatments possess different letters, one can conclude that their means are significantly different from each other; conversely, if the letters match, their means are not statistically different.

For stiffness, even though the highest value appears at 3.59 g/100 g solids moisture content, it does not deviate significantly from the stiffness values at 3.74 and 8.53 g/100 g solids moisture content. The latter two treatments also equate to those in the b group (i.e., 6.41, 3.89, 3.86, 3.37, and 2.71 g/100 g solids moisture content) but different from the two lowest stiffness values with the group title of d and c. For hardness, although the 8.53 and 6.41 g/100 g solids samples display the top two highest values, both treatments are statistically equal to that of the 3.62 g/100 g solids. At the same time, treatment 8 is not significantly different from the samples within group b (including 9.71, 3.89, 3.86, 3.74, 3.59, 3.37, and 2.71 g/100 g solids) but markedly differs from the lowest hardness value at 12.26 g/100 g solids moisture content. Finally, for Young's modulus, the three higher values, which correspond to the moisture content values of 8.53, 6.41, and 3.59 g/100 g solids, align statistically with the 3.89, 3.86, 3.74, and 3.62 g/100 g solids moisture content. Meanwhile, the latter treatments are equal to the 9.71, 3.37, and 2.71 g/100 g solids samples within group b. In addition, treatment 1 with the label c suggests a different Young's modulus value compared to those with labels a, b, and ab.

Table 2 The result of ANOVA for different micromechanical values, at a significance level of 0.05

Statistical parameter	Stiffness	Hardness	Young's modulus
P-value	< 0.0001	< 0.0001	< 0.0001
F-value	21.29	12.65	21.23
Degrees of freedom between groups	10	10	10

Conclusions

Nanoindentation was employed in this study to measure the micromechanical properties changes of cookie samples during the baking process. It was concluded that while moisture influences the micromechanical properties of cookies, it is not the exclusive determinant of hardness, stiffness, and Young's modulus values. The considerable dependence of properties on moisture content was only observed for cookie samples with moisture content greater than 8.5 g/100 g solids. For lower moisture content, there are fluctuations in the trends of micro-level mechanical properties that are expected to be due to other potential factors like pore structure changes and fat displacement. The highest values for hardness and Young's modulus were achieved at a moisture content of 8.53 g/100 g solids, while the highest value of stiffness takes place at a moisture content of 3.59 g/100 g solids. The indicated moisture content values are expected to provide cookies that are more prone to resist mechanical damage during handling and transport due to higher hardness, Young's modulus and stiffness values. However, one

Table 3 Duncan's multiple range test for stiffness, hardness and Young's modulus of samples at different moisture content values at a 5% probability (mean of replicates ± standard deviation (SD)).

Treatment	Baking time (min)	Moisture content (g/100 g solids) ± SD	Stiffness (µN/nm) ± SD	Hardness (GPa) ± SD	Young's modulus (GPa) ± SD
TRT 1	10	12.26 ± 0.13	9.77 ± 1.70^{d}	0.28 ± 0.07^{c}	4.34 ± 0.66^{c}
TRT 2	15	9.71 ± 0.42	16.06 ± 1.69^{c}	0.71 ± 0.09^{b}	11.47 ± 1.80^{b}
TRT 3	20	8.53 ± 0.14	18.56 ± 1.56^{ab}	0.88 ± 0.22^{a}	14.55 ± 2.24^{a}
TRT 4	25	6.41 ± 0.08	18.32 ± 1.86^{b}	0.86 ± 0.24^{a}	14.12 ± 2.38^{a}
TRT 5	30	3.89 ± 0.01	18.13 ± 2.86^{b}	0.71 ± 0.1^{b}	12.85 ± 2.29^{ab}
TRT 6	35	3.86 ± 0.03	18.06 ± 1.34^{b}	0.69 ± 0.15^{b}	12.63 ± 1.79^{ab}
TRT 7	40	3.74 ± 0.07	18.91 ± 1.87^{ab}	0.68 ± 0.14^{b}	13.13 ± 2.18^{ab}
TRT 8	45	3.62 ± 0.23	17.15 ± 2.22^{bc}	0.77 ± 0.13^{ab}	12.66 ± 2.36^{ab}
TRT 9	50	3.59 ± 0.42	20.16 ± 2.71^{a}	0.70 ± 0.17^{b}	14.22 ± 2.94^{a}
TRT 10	55	3.37 ± 0.09	17.97 ± 2.23^{b}	0.64 ± 0.12^{b}	12.01 ± 1.28^{b}
TRT 11	60	2.71 ± 0.08	17.92 ± 1.82^{b}	0.63 ± 0.14^{b}	11.98 ± 2.14^{b}

Significant differences between means are demonstrated by Duncan's grouping letters (a to d) from the highest (a) to lowest (d) mean value also needs to account for taste acceptability and mouthfeel for given moisture content in future studies. ANOVA indicates a significant difference for each of the micromechanical properties at different moisture content values, and Duncan's multiple range test grouped samples from 12.26 to 2.71 g/100 g solids in different categories having no significant differences, except the samples of TRT 1, so that the optimum sample can be selected with more flexibility. In this study, the nanoindentation technique was found to be an effective tool for estimating how a cookie's mechanical properties change on a microscale throughout baking. The collected data would help the cookie industry in developing a high-quality product by desirably controlling the micromechanical properties by adjusting the baking process parameters.

Acknowledgements Thanks to the Center for Advanced Research in Drying (CARD) and the National Science Foundation (NSF) for providing financial support under award number 1624812.

Author contributions Karla Cecilia Cisneros Martinez: methodology, material preparation, data collection and analysis, writing-original draft preparation, editing. Ramin Nemati: methodology, material preparation, data analysis, writing-original draft preparation and review, editing. Pawan Singh Takhar: Conceptualization, writing-review and editing, funding acquisition and supervision.

Data availability Data is available upon request to the corresponding author.

Declarations

Conflict of interest The authors declare no conflict of interest.

References

1. N.N. Misra, B.K. Tiwari, in *Bak. Prod. Sci. Technol*, edited by W. Zhou, Y. H. Hui, I. De Leyn, M. A. Pagani, C. M. Rosell, J. D. Selman, and N. Therdthai (John Wiley & Sons, Ltd, 2014), pp. 585–601
2. T. Lucas, in *Bak. Prod. Sci. Technol*, edited by W. Zhou, Y. H. Hui, I. De Leyn, M. A. Pagani, C. M. Rosell, and N. Therdthai (John Wiley & Sons, Ltd, 2014), pp. 335–354
3. M. Krokida, Z. Maroulis, in *Dry. Technol. Agric. Food Sci*, edited by A. S. Mujumdar (2000), pp. 61–68
4. P.J. Fellows, in *Food Process. Technol. Fourth Ed*, edited by P. J. FellowsWoodhead Publishing, (2017), pp. 3–200
5. R. Lu, in *Instrum. Assess. Food Sens. Qual*, edited by D. Kilcast-Woodhead Publishing, (2013), pp. 103–128
6. J.M. Aguilera, J. Food Eng. **67**, 3 (2005)
7. J. Parada, J. Aguilera, J. Food Sci. **72**, R21 (2007)
8. S. Davis, J. Zekonyte, A. Karali, M. Roldo, G. Blunn, Bioengineering. **10**, 995 (2023)
9. D.M. Ebenstein, L.A. Pruitt, Nano Today. **1**, 26 (2006)
10. A. C. *Fischer-Cripps, Nanoindentation* (Springer, New York, NY, 2004)
11. A. C. *Fischer-Cripps, Nanoindentation* (Springer, New York, NY, 2011)
12. X. Rao, F. Zhang, X. Luo, F. Ding, Mater. Sci. Eng. **744**, 426 (2019)
13. A. Sinha, A. Bhargav, Mech. Ind. **21**, 404 (2020)
14. G. Kimbell, M.A. Azad, in *Bioinspired Biomim. Mater. Drug Deliv*, edited by M. NurunnabiWoodhead Publishing, (2021), pp. 295–318
15. A. Baiano, A. Di Chio, D. Scapola, Qual. Assur. Saf. Crops Foods 11, 713 (2019)
16. A. Rzigue, J.-Y. Monteau, K. Marmi, A. Le Bail, S. Chevallier, A.-L. Réguerre, V. Jury, J. Food Eng. **182**, 72 (2016)
17. S.H. Williams, B.W. Wright, V. den Truong, C.R. Daubert, C.J. Vinyard, Am. J. Primatol. **67**, 329 (2005)
18. M.T. Mansour, K. Tsongas, D. Tzetzis, J. Compos. Sci. **5**, 62 (2021)
19. J. Miao, T. Li, Q. Li, X. Chen, Z. Ren, Y. Lu, Materials. **16**, 1085 (2023)
20. X. Sun, L. Li, Y. Guo, H. Zhao, S. Zhang, Y. Yu, D. Wu, H. Liu, M. Yu, D. Shi, Z. Liu, M. Zhou, L. Ren, L. Fu, AIP Adv. **8**, 035003 (2018)
21. M. Yamamoto, M. Tanaka, O. Furukimi, Materials. **14**, 7217 (2021)
22. H. Jabir, A. Fillon, P. Castany, T. Gloriant, Phys. Rev. Mater. **3**, 063608 (2019)
23. J. Wei, Z. Ma, H. Wen, H. Guo, J. Tang, J. Liu, Y. Li, Y. Sugawara, Coatings. **10**, 84 (2020)
24. R. Hiesgen, S. Helmly, I. Galm, T. Morawietz, M. Handl, K.A. Friedrich, Membranes. **2**, 783 (2012)
25. T. Hassenkam, L.L. Skovbjerg, S.L.S. Stipp, Proc. Natl. Acad. Sci. 106, 6071 (2009)
26. S.K. Enganati, F. Addiego, J.P.C. Fernandes, Y. Koutsawa, B. Zielinski, D. Ruch, G. Mertz, Polym. Test. **98**, 107203 (2021)
27. C.R. Jones, Z.J. Zhang, H.-J. Tsai, Methods Mol. Biol. Clifton NJ. **2667**, 1 (2023)
28. M. Griepentrog, G. Krämer, B. Cappella, Polym. Test. **32**, 455 (2013)
29. I. Rosenhek-Goldian, S.R. Cohen, J. Vac Sci. Technol. A **41**, 062801 (2023)
30. L. Kong, F. Hadavimoghaddam, C. Li, K. Liu, B. Liu, A. Semnani, M. Ostadhassan, Mar. Pet. Geol. **132**, 105229 (2021)
31. A. Zdunek, A. Kurenda, Sensors. **13**, 12175 (2013)
32. R. Khodabakhshian, A. Naeemi, M.R. Bayati, J. Texture Stud. **52**, 389 (2021)
33. A. Zdunek, A. Kozioł, J. Cybulska, M. Lekka, P.M. Pieczywek, Planta. **243**, 519 (2016)
34. S. Cárdenas-Pérez, J.J. Chanona-Pérez, J.V. Méndez-Méndez, G. Calderón-Domínguez, R. López-Santiago, I. Arzate-Vázquez, Innov. Food Sci. Emerg. Technol. **34**, 234 (2016)
35. S. Cárdenas-Pérez, J.V. Méndez-Méndez, J.J. Chanona-Pérez, A. Zdunek, N. Güemes-Vera, G. Calderón-Domínguez, F. Rodríguez-González, Innov. Food Sci. Emerg. Technol. **39**, 79 (2017)
36. M. Escamilla-García, G. Calderón-Domínguez, J.J. Chanona-Pérez, R.R. Farrera-Rebollo, J.A. Andraca-Adame, I. Arzate-Vázquez, J.V. Mendez-Mendez, L.A. Moreno-Ruiz, Int. J. Biol. Macromol. **61**, 196 (2013)
37. M. Escamilla-García, A. Reyes-Basurto, B.E. García-Almendárez, E. Hernández-Hernández, G. Calderón-Domínguez, G. Rossi-Márquez, C Regalado-González Coat. **7**, 224 (2017)
38. L. Severa, J. Němeček, Š. Nedomová, J. Buchar, J. Food Eng. **101**, 146 (2010)
39. K. Dhalsamant, P.P. Tripathy, S.L. Shrivastava, J. Sci. Food Agric. **97**, 3312 (2017)
40. I.H. Md., N. Khan, M. Patel, Mahiuddin, M.A. Karim, J. Food Eng. **291**, 110306 (2021)
41. S. Wang, H. Zhao, Micromachines. **11**, 407 (2020)
42. B. Bhushan, M.L.B. Palacio, in *Encycl. Nanotechnol*, edited by B. BhushanSpringer Netherlands, Dordrecht, (2016), pp. 2423–2444

43. W.C. Oliver, G.M. Pharr, J. Mater. Res. **7**, 1564 (1992)
44. H. Wang, L. Zhu, B. Xu, in *Residual Stress. Nanoindentation Test. Films Coat*, edited by H. Wang, L. Zhu, and B. XuSpringer, Singapore, (2018), pp. 21–36
45. B. Bhushan, M.L.B. Palacio, in *Encycl. Nanotechnol*, edited by B. BhushanSpringer Netherlands, Dordrecht, (2012), pp. 1576–1596
46. J. Gong, B. Deng, H. Qiu, D. Jiang, Mater. Chem. Phys. **251**, 123165 (2020)
47. T. Iqbal, B.J. Briscoe, P.F. Luckham, Eur. Polym. J. **47**, 2244 (2011)
48. K.K. Jha, N. Suksawang, D. Lahiri, A. Agarwal, J. Mater. Res. **28**, 789 (2013)
49. M. Liu, C. Lu, K. Tieu, H. Yu, Mater. Sci. Eng. A **619**, 57 (2014)
50. J. Čech, P. Haušild, O. Kovářík, A. Materna, Mater. Des. **109**, 347 (2016)
51. C. Jin, Z. Wang, A.A. Volinsky, A. Sharfeddin, N.D. Gallant, Polym. Test. **56**, 329 (2016)
52. A.K. Sikder, Proc. Inst. Mech. Eng. Part J J. Eng. Tribol. 235, 1075 (2021)
53. K.O. Kese, A.-M. Alvarez, J.K.-H. Karlsson, K.H. Nilsson, J. Nucl. Mater. **507**, 267 (2018)
54. J. Wang, C. Yang, Y. Liu, Y. Li, Y. Xiong, ACS Omega. **7**, 14317 (2022)
55. E.E. Finney, J. Agric. Eng. Res. **12**, 249 (1967)
56. M. Molenda, M. Stasiak, Int. Agrophysics **16**, (2002)
57. AACC, *Approved Methods of the American Association of Cereal Chemists* (AACC, 2000)
58. L. Ameur, O. Mathieu, V. Lalanne, G. Trystram, I. Birlouezaragon, Food Chem. **101**, 1407 (2007)
59. S. Chevallier, G. Della Valle, P. Colonna, B. Broyart, G. Trystram, J. Cereal Sci. **35**, 1 (2002)
60. I. Konopka, D. Rotkiewicz, M. Tańska, Eur. Food Res. Technol. **220**, 20 (2005)
61. H. Qin, D. Ma, X. Huang, J. Zhang, W. Sun, G. Hou, C. Wang, T. Guo, Crop J. **7**, 19 (2019)
62. E.A. Asamoah, A. Le-Bail, A. Oge, D. Queveau, O. Rouaud, and P. Le-Bail, Foods 12, 946 (2023)
63. G. Pop, J. Agroaliment Process. Technol. XIII, 105 (2007)
64. M.U.H. Joardder, A. Karim, C. Kumar, R.J. Brown, *Porosity: Establishing the Relationship between Drying Parameters and Dried Food Quality* (Springer International Publishing, Cham, 2016)
65. R.S. Uysal, G. Sumnu, I.H. Boyaci, J. Food Process. Eng. **42**, e12977 (2019)
66. M. Kurniadi, Y. Khasanah, A. Kusumaningrum, M. Angwar, D. Rachmawanti, N.H.R. Parnanto, L.D. Pratiwi, Earth Environ. Sci. **251**, 012034 (2019). IOP Conf. Ser
67. M. Nugraheni, S. Sutopo, S. Purwanti, and T. Widi Handayani, Food Res. 658 (2019)
68. B. Asefa, Food Sci. Qual. Manag. **65**, 16 (2017)
69. M. Suriya, R. Rajput, C.K. Reddy, S. Haripriya, M. Bashir, J. Food Sci. Technol. **54**, 2156 (2017)
70. A.B.D. Nandiyanto, R. Ragadhita, A. Ana, B. Hammouti, Int. J. Technol. **13**, 432 (2022)
71. I. Rombouts, B. Lagrain, K. Brijs, J.A. Delcour, Amino Acids. **42**, 2429 (2012)
72. D. Mohan, M.S. Sajab, H. Kaco, S.B. Bakarudin, Mohamed Noor Nanomaterials. **9**, 1726 (2019)

Publisher's Note Springer Nature remains neutral with regard to jurisdictional claims in published maps and institutional affiliations.

Springer Nature or its licensor (e.g. a society or other partner) holds exclusive rights to this article under a publishing agreement with the author(s) or other rightsholder(s); author self-archiving of the accepted manuscript version of this article is solely governed by the terms of such publishing agreement and applicable law.